The Charles Stark Draper Laboratory, Inc.
555 Technology Square, Cambridge, Massachusetts 02139 Telephone (617) 258-

Space Station-86-19

TO: Distribution

FROM: J. Paradiso

DATE: December 1, 1986

SUBJECT: Selection and Management of Magnetically Gimballed CARES Gyroscopes via Linear Programming

I) Introduction

This report summarizes the results of an initial effort performed to adapt the linear programming based CMG selection/steering procedure[1,2] to manage Draper-developed, magnetically suspended CARES (Combined Attitude, Reference, and Energy Storage) gyroscopes[3]. The first section documents the approach taken in modelling the device to enable linear programming selection. The following section describes how constraints on peak gimballing rate and gimbal angular freedom were accomodated. The final section of this report presents a series of simulation examples investigating the response of a CARES system controlling a proposed experimental SDI mirror platform[4]. The details of the linear selection method and vehicle controllers applied here are discussed in Refs. 1 and 2; it is assumed that the reader is somewhat familiar with these concepts.

II) Modelling Strategy

A simplified schematic defining conventions used in describing the CARES system is shown in Fig. 1. The CARES gyro generates an output torque by changing the angular orientation of its rotor, as is performed by a conventional CMG system (output torque may also be generated in standard reaction wheel fashion by changing the rotor rate; although this option could also be incorporated into the linear programming scheme, it

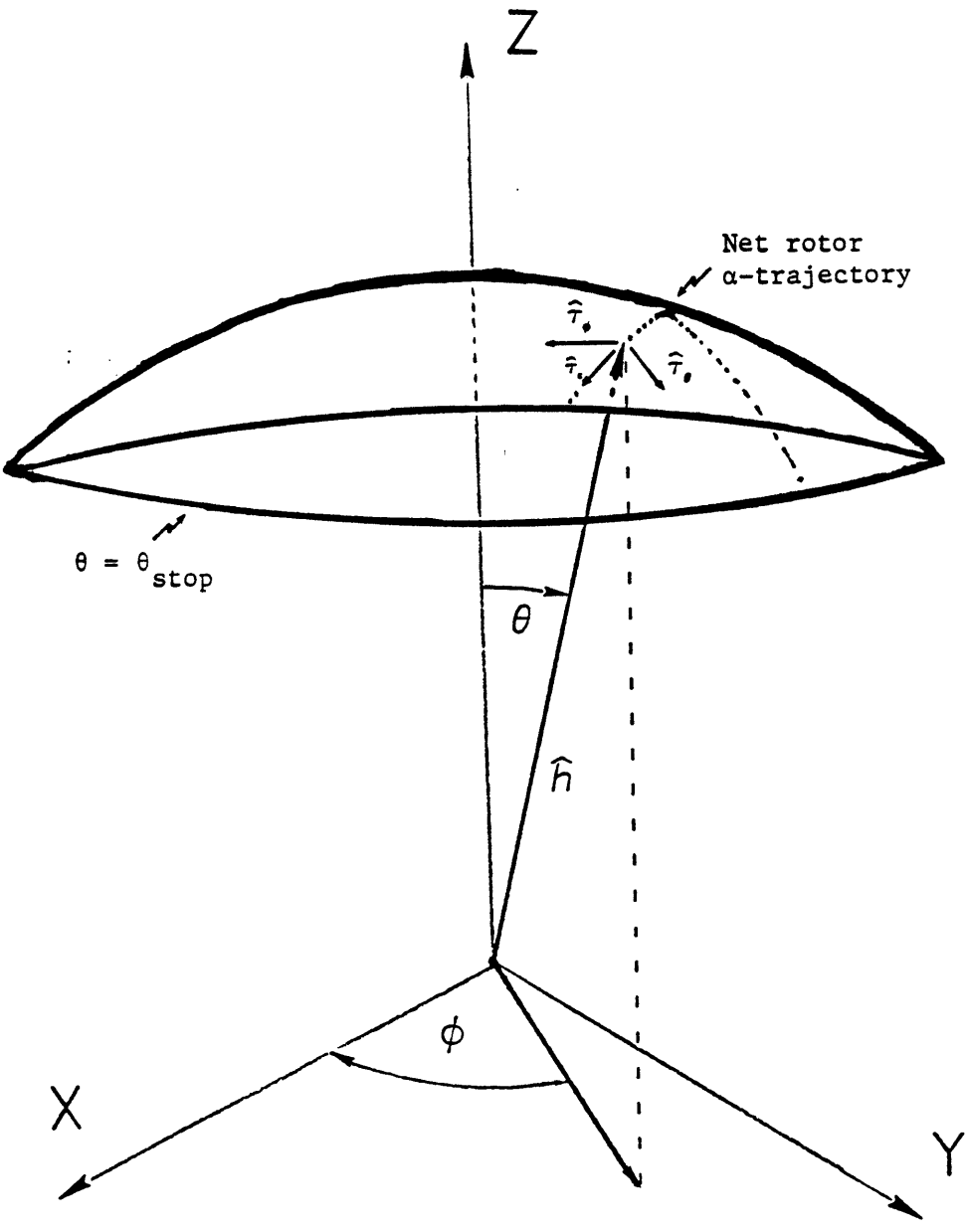

NOTE: Reaction Torques on the Vehicle are Directed Opposite to the vectors $\hat{\tau}$ specified here.

FIGURE 1: CARES Schematic and Coordinate Definition

has not been addressed by this initial study). Conventional CMG rotors are mounted on gimbals which fix their rotational freedom, and each CMG gimbal is independently constrained to rotate below a maximum rate. The CARES system, however, uses a magnetically suspended rotor, thus the rotation is not fixed by a gimbal mount, and the rotor may generally be moved in any direction. In this situation, the net rotor motion (as opposed to its projection along a particular gimbal axis) is constrained to remain under a maximum rate.

The coordinate convention used in describing the CARES system is illustrated in Fig. 1. The position of the rotor ($\hat{h}$) is determined by a polar angle (θ) and azimuth angle (ϕ). The hardware required for magnetic suspension results in a tight limit on the allowable rotor excursion in the polar coordinate; $\theta<15°$ is typically enforced (the ability of linear programming to specify upper bounds on rotor motion is particularly well-suited to this restriction). The situation is illustrated in Fig. 1, where the rotor is allowed to point anywhere in the bowl-like region with $\theta<\theta_{stop}$.

In order to allow the linear program to select both the direction and rate of rotor displacement, two orthogonal activity vectors are specified for each CARES rotor; one generating displacement in the polar direction ($\hat{\tau}_\theta$) and the other generating displacement in the azimuthal direction ($\hat{\tau}_\phi$). The linear program selects these activity vectors in response to an input vehicle rate-change or torque command, assigning them decision variables a_θ and a_ϕ (these represent angular displacements when solving for a vehicle rate-change, or angular rates when solving for a vehicle torque). The resulting rotor motion is described by:

1)
$$\hat{\tau}_c = \text{unit}(a_\theta \hat{\tau}_\phi + a_\phi \hat{\tau}_\phi)$$

$$a_c = \sqrt{a_\theta^2 + a_\phi^2}$$

(The hat "^" denotes a unit vector)

The vector $\hat{\tau}_c$ represents the instantaneous direction of rotor displacement specified by the selection routine, and a_c is its amplitude (ie. net angular displacement or rate). After a selection is performed, the CARES environment simulation steps the rotor position along the circle centered at the origin with tangential vector $\hat{\tau}_c$ (the axis of rotation is defined by $\hat{h} \times \hat{\tau}_c$, and the rotor path is denoted by the dotted curve plotted in Fig. 1). Resulting vehicle reaction torques are calculated, and the vehicle state is updated accordingly. The location of the stop limit along this trajectory is calculated as defined by:

$$2) \qquad \alpha_{stop} = +/- \cos^{-1}\left[\frac{\cos \theta_{stop}}{\cos \theta_o}\right]$$

where α is the rotor angular displacement along the composite curve referenced to $\alpha=0$ when $\hat{h}$ is at closest approach to the z-axis (the value of θ at this point, defined by θ_o, is the minimum over the entire rotor trajectory). If an attempt is made to move a rotor past its stop, the environment software places the rotor exactly at the stop limit (ie. $\alpha=\alpha_{stop}$ on the composite trajectory), and ceases incrementing the rotor displacement until the next CARES selection is performed.

Because of the linear tangent approximation made to the device output torque, the CARES selection must be repeated after the rotors have moved across a preset displacement. New $\hat{\tau}_\phi$ and $\hat{\tau}_\theta$ vectors are generated at the updated rotor position, and another selection is performed to generate $\hat{\tau}_c$ and a_c, thereby specifying a revised rotor trajectory.

By aligning the outer gimbal axis with $\hat{z}$ (see Fig. 1) and defining inner gimbal angle $\gamma'=90°-\gamma$, the coordinate system and rotation algorithms developed for double gimballed CMGs (eg. Sec. 2.5 and Fig. 10 of Ref. 2) were adapted to describe the rotor position of the CARES device. In this fashion, the "inner gimbal angle" γ' becomes the polar angle θ, and the outer gimbal angle α is equal to the azimuthal angle ϕ. By defining this relationship, much of the logic used in the CMG steering law to calculate activity vectors, torques, objective factors, etc. can be applied to CARES without extensive adaptation.

The calculation of objective factors is described in Chapter 3 of Ref. 2. The three terms (minimization of inner gimbal [ie. polar] angle, stops avoidance, and rotor lineup repulsion) were implimented essentially as discussed in Ref. 2. The stops objective contribution for ϕ-displacement was modified somewhat to account for the fact that traversal in either direction along the trajectory associated with $\hat{\tau}_\phi$ can also lead toward maximum θ (remember that this rotation is about a great circle centered at the origin, not about a latitude curve). This was accomplished by setting both stops objective coefficents associated with $\hat{\tau}_\phi$ to be equal to the stops objective contribution associated with increasing θ. Because of this, the only activity vector which has zero associated stops objective is that corresponding to rotor displacement in the negative $\hat{\tau}_\theta$ direction; this is the only activity in these coordinates which can move the rotor away from the stop limit, thus it becomes increasingly favored as the rotor approaches the stop.

III) Accomodation of Hardware Constraints

By imposing upper bounds on the useage of CARES activity vectors (ie. limiting a_θ and a_ϕ independently in positive and negative directions), the linear program has the ability to directly incorporate hardware constraints such as stop locations and maximum gimballing rates. Because of dimensional differences, the calculation of upper bounds is performed differently when solving for commanded vehicle rate-changes and vehicle torques. Each situation is discussed independently below:

1) Rate-Change Commands

In this case, the calculated decision variables a_θ and a_ϕ represent rotor displacements along the directions dictated by their associated activity vectors. All a_c for composite rotor displacement are calculated by summing each set of a_θ and a_ϕ in quadrature (as in Eq. 1). The maximum a_c thus obtained is normalized to the peak

gimballing rate (as in Eq. 27 of Ref. 2) such that the corresponding rotor (which travels the farthest) is moved at maximum speed, with all others travelling at lower rates proportional to their relative a_c values. Because of this normalization, the peak gimballing rate is never exceeded, although it also becomes impossible to directly command or control the level of output torque, since it is determined by the normalization procedure.

The upper bound values imposed on a_θ and a_ϕ now represent maximum allowed gimbal displacements along the directions specified by their associated activity vectors. The logic applied here is again very similar to that used for CMGs in Sec. 2.5 (ie. Eq. 29) of Ref. 2. The upper bound on a_θ is equal to the angle remaining between the rotor and the stop (ie. $\theta_{stop}-\theta$) for displacements which increase θ (ie. $+\hat{\tau}_\theta$). Displacements in the opposite direction are bounded by either $2\theta_{stop}-\theta$ or the generic clamp "L" (See Eq. 29 Ref. 2). Traversal along the azimuthal (ϕ) direction also approaches the stops; the distance from the current rotor position to the stop limit along ϕ in either direction is defined by Eq. 2 (replacing θ_o with the current polar angle θ); this quantity is used as the upper bound on a_ϕ in both directions.

Since the actual net rotor displacement is defined by the quadrature sum of independent displacements along two orthogonal axes, this method of bounding each component of rotor displacement individually does not necessarily guarantee that the composite solution (a_c and $\hat{\tau}_c$) will always keep the rotor inside the stops. Although it may be imprecise, independently upper bounding the activity vectors in this way is still useful in that it informs the selection procedure of the increasingly limited freedom available as rotors are moved toward their stops. Since the vehicle environment software is structured to prevent a rotor from passing a stop (certainly a feature implemented in actual hardware), solutions which attempt to pass stop limits are revised after a rotor reaches a stop, and all of the corresponding upper bounds in the subsequent selection are set to zero (preventing related rotor motion), except for the bound which dictates rotation along $-\hat{\tau}_\theta$ (this is the only direction which pulls the rotor away from the stop).

2) Torque Commands

In this case, the a_θ and a_ϕ output by simplex represent actual gimballing rates projected along each coordinate. They are summed in quadrature to form the net gimballing rate (a_c) along $\hat{\tau}_c$, as in Eq. 1. These gimballing rates are used directly (without normalization as needed above in the rate-change case), since the a_θ and a_ϕ are bounded such that their quadrature sum a_c does not exceed the allowed maximum value. Two independent strategies have been pursued in order to accomplish this goal. The first is a simple "brute force" method of bounding each decision variable a_θ and a_ϕ by the the maximum composite gimballing rate divided by $\sqrt{2}$:

$$3) \qquad a_\theta, a_\phi < \frac{a_{cm}}{\sqrt{2}}$$

This approach guarantees that a_c will always be less than or equal to its maximum value a_{cm}. For solutions which require large control authority about one of the coordinate axes, however, this bounding policy becomes restrictive, and the actuator is only able to project up to 71% of its full torque potential along the desired direction.

Another method was pursued in an attempt to rectify this problem. The initial upper bounds on both a_θ and a_ϕ were set at the correlated maximum (a_{cm}), enabling simplex to exploit the full actuator torque authority along any axis. If, during the course of simplex operations, a CARES activity vector was invited into the basis (ie. direction $\hat{\tau}_\theta$ was invited with gimballing rate a_θ), the bound on the correlated decision variable (termed u_ϕ in this example) must be correspondingly decreased

$$4) \qquad a_\theta < \sqrt{a_{cm}^2 - a_\theta^2} \equiv u_\phi$$

If the activity vector corresponding to $\hat{\tau}_\theta$ is again excluded from the solution (ie. a_θ is set to zero), the upper bound u_ϕ is restored again to its maximum value a_{cm}. In this fashion, the values of the

upper bounds on CARES activity vectors are dynamically adjusted throughout the simplex procedure in order that the quadrature sum of each activity vector pair (a_c) does not exceed its maximum (a_{cm}).

In practice, this procedure must be implemented in a somewhat more complex fashion. Before every simplex operation, the following list of conditions must be checked. The notation defined in Sec. 2.4 of Ref. 2 is used below, and the term "partner" denotes a companion activity vector (ie. corresponding θ or ϕ vector to the rotor considered). In the following equations, a_i denotes the decision variable of the invited activity vector.

a) Partner of invited activity vector is in the basis:

5) $$\sqrt{a_i^2 + (-T_j a_i + a_j)^2} < a_{cm}$$

a_j = Decision variable of invited activity vector's partner in the basis

$-T_j$ = Varience of a_j with invited a_i (see Ref. 2)

b) Partner of invited activity vector is at upper bound:

6) $$\sqrt{a_i^2 + a_{j(ub)}^2} < a_{cm}$$

$a_{j(ub)}$ = Decision variable of invited activity vector's partner at upper bound

c) Two partners are simultaneously in the basis:

7) $$\sqrt{(-T_j a_i + a_j)^2 + (-T_k a_i + a_k)^2} < a_{cm}$$

a_j, a_k = Decision variables of the two partners in the basis

d) Partner of a basic activity vector is at upper bound:

8) $$\sqrt{(-T_j a_i + a_j)^2 + a_{k(ub)}^2} < a_{cm}$$

$a_{k(ub)}$ = Upper bounded decision variable associated with the partner of the basic variable a_j

Before every simplex operation (ie. pivot, upper bounding) is executed, all occurances of situations a through d must be investigated. This check is performed by solving Eqs. 5 through 8 for a_i (the quadratic formula may be used) wherever the corresponding situation exists. If the minimum a_i imposed by these conditions is less than X_UB_BEST or $UBOUND_{INVITE}$ (these denote limits on the invited decision variable imposed by the conventional non-correlated upper bounding logic; see Sec. 2.4 of Ref. 2), the appropriate quantity is replaced. If the minimum a_i replaces U_BOUND_{INVITE}, the invited activity vector will be placed at its upper bound; if it replaces X_UB_BEST, a basic partner which hits its correlation limit (index stored in L_UB) is removed from the basis and placed at its upper bound.

If an activity vector has been placed at a "correlation bound", as defined above, a flag is set to distinguish it from other activity vectors placed at conventional upper bounds. Whenever the decision variable corresponding to the partner of an activity vector at a correlation bound is decreased by a simplex operation, the correlation bound is effectively reset, and simplex is again allowed to increase the magnitude of either decision variable in subsequent operations. In the case (c), with two partners simultaneously cohabiting the basis, a correlation limit will cause one of them (the vector with the largest variance $|T_j|$ is chosen) to be removed from the basis and upper bounded. Both partners, however, are effectively locked from increasing and its decision variable can not be increased. If the next simplex operation does not decrease the decision value of this remaining partner, it must also be pivoted out of the basis and placed it also at its limit (via condition d).

This method allows simplex to dynamically adapt itself to a problem as it is being solved, and prevents correlation limits from ever being exceeded, while still allowing the selection process access to the full torque potential of each actuator. Because of the sequential nature of simplex, however, the latter claim is not always maintained. When faced with a very large input torque command, the initial simplex operations will place several activity vectors at their upper bounds. Subsequent

operations will swap and adjust basic decision variables such that an optimal solution is achieved. Because of the correlation constraints, however, activity vectors placed at thier initial upper bounds (a_{cm}) prevent their partner vectors from being used at all. Because simplex essentially manages only one set of activity vectors at a time (ie. an invited and excluded vector in a swap or bounding operation), it is generally unable to adjust both correlated activity vectors simultaneously. This can cause simplex to lock into solutions with pairs of partners placed at correlation limits; the pivoting operation is not always able to "unlock" these pairs in order to proceed to other solutions. This is illustrated in the example mentioned above; ie. solutions to large input commands are generally characterized by individual activity vectors (representing rotor displacements in the $\hat{\tau}_\theta$ and $\hat{\tau}_\phi$ directions) at correlation bounds (a_{cm}) and their partners at zero. For commands which project primarily onto the $\hat{\tau}_\theta$ or $\hat{\tau}_\phi$ coordinates, the maximum control authority yielded by this strategy will indeed be aligned with the desired axes. In the more general situation, however, when commands project between $\hat{\tau}_\theta$ and $\hat{\tau}_\phi$, these solutions are not necessarily able to direct the maximum actuator authority along the commanded axis, potentially causing premature torque saturation.

This method of dynamic correlation bounding causes an effect converse to that observed using the technique described earlier, where each activity vector was independently limited to $a_{cm}/\sqrt{2}$. That method favored commands which projected equally along each actuator axis, while this technique favors commands projecting onto single coordinate axes. One might extend the former concept by tailoring the actuator bounds to the orientation of the input command before starting simplex (thus bounding a_θ and a_ϕ differently, depending upon the commanded direction). The dynamic nature of the correlation bounding technique, however, holds considerable promise in that it potentially allows simplex to continually adapt as it solves a problem. This method initially places minimal restrictions on the system, and allows simplex to balance correlated activity vectors as it sees fit. Provided that one could originate a means of relieving pivoting impasses caused by correlated

bounds, it could become a powerful and general technique for commanding actuators constrained in this manner.

Because the decision variables calculated in response to torque commands represent gimballing rates (and not angular displacements), gimbal stops may be only indirectly incorporated into any bounding strategy. Displacement limits are currently implemented by creating a "soft stop", where the upper bounds corresponding to rotor motion toward the stop are linearly decreased after the rotor approaches the stop vicinity to within a preset distance (typically 1° in this case), effectively limiting the actuator control authority available in that direction. By the time a rotor reaches a stop, its bounds in directions that would move it past the stop are set to zero (preventing such simplex selection), and the bound corresponding to motion away from the stop ($-\hat{\tau}_\theta$) remains at its quiescent value (allowing its activity vector to be selected by simplex). This technique is compatable with either of the gimballing rate bounding strategies detailed above.

IV) Simulation Examples

The assumptions and techniques described above were applied in simulations investigating vehicle control achieved through a set of CARES gyros. A system of four CARES rotors are assumed to be mounted as portrayed in Fig. 2, with two momenta pointing up (along +yaw) and two pointing down (along -yaw). The rotors are initially displaced from the yaw axis by 5 degs. in polar angle (θ) and are rotated in azimuth (ϕ) such that the upper two are inclined toward the +roll and -pitch axes, while the lower two are inclined toward -roll and +pitch. This results in a zero momentum initial state possessing finite control authority about the yaw axis. The vehicle is based upon an experimental SDI orbital mirror[4]; the mirror is modelled as a thin disk, with the yaw axis at its center (because mission requirements for this spacecraft will entail rapid slews about pitch and roll, maximum control authority is required in the pitch/roll plane, thus the CARES rotors are mounted along the yaw axis). The CARES parameters were set according to Ref. 5; ie.

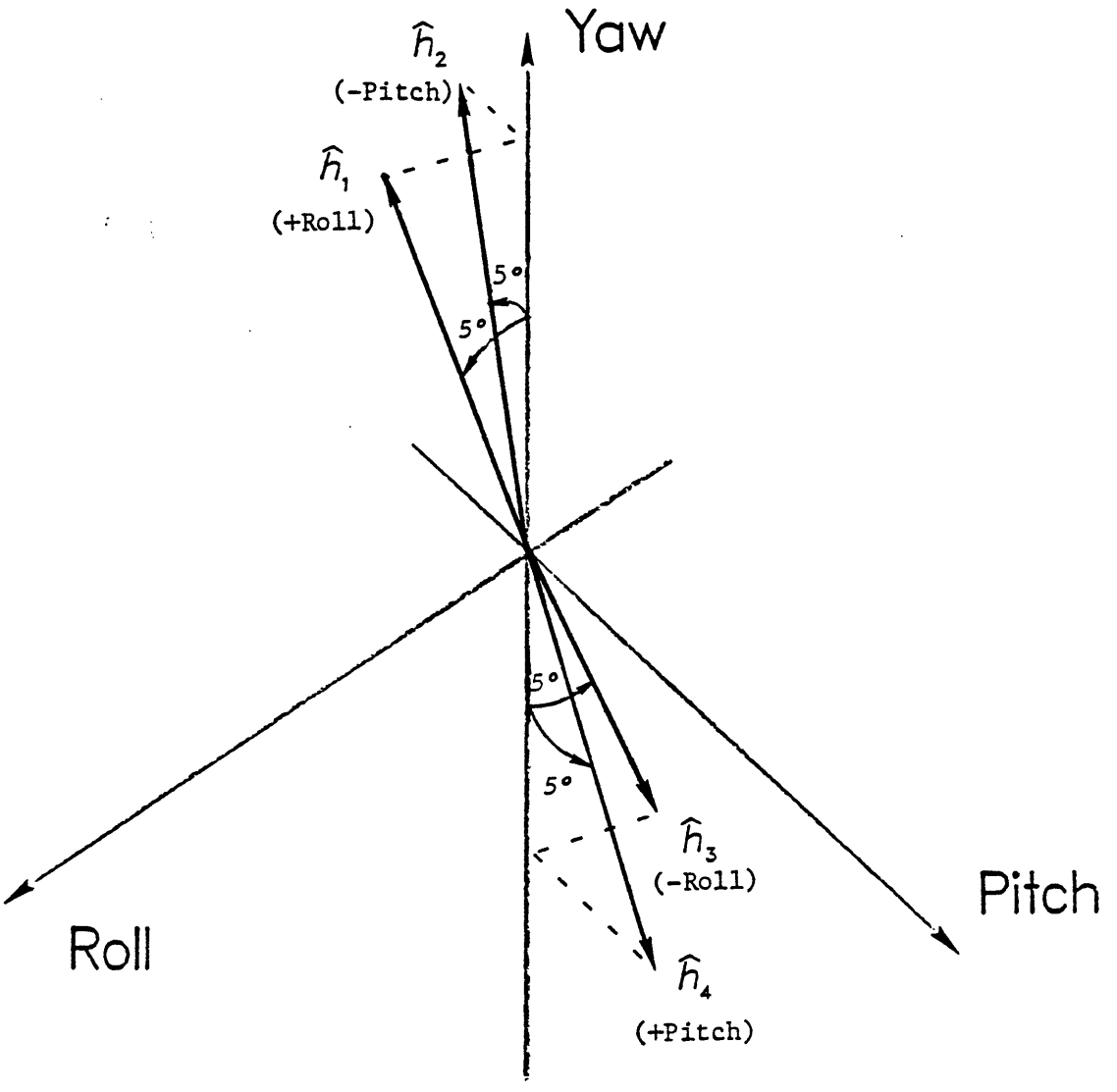

FIGURE 2: CARES Mounting Scheme and Initial Rotor Orientation

each rotor stores 2500 ft-lb-sec of angular momentum (the value quoted in Ref. 5 was misprinted to be a factor of ten too large), maximum gimballing rates (a_{cm}) are 0.25 rad/sec, and allowed gimbal travel is $\theta<15°$. The vehicle moments of inertia (contributions from CARES are ignored) are assumed to be 3000 slug-ft^2 about the yaw axis and 1500 slug-ft^2 each about pitch and roll (the large ratio of stored actuator momentum to vehicle inertia arises from the rapid vehicle response needed for quick re-targeting coupled with the stringent 15° limit on rotor displacement). Rigid-body assumptions and simple kinematics are used to calculate the CARES response and output torques. While much would be learned by applying a dynamic CARES model, such an effort is beyond the scope of this task.

The rate-feedback controller described in Chapter 5 of Ref. 2 has been adapted to drive the CARES linear selection with a torque request proportional to the desired rate change (this torque is saturated at a minimum value for small rate-change inputs in order to maintain prompt the linear CARES selection; the commanded rate-change mode is not used in these tests. Both gimballing rate bounding strategies discussed earlier are applied in a "hybrid" approach; simplex first bounds all CARES activity vectors by $a_{cm}/\sqrt{2}$, and if imaginary activity vectors appear in the solution (indicating saturation), all bounds are reset to a_{cm}, and simplex attempts to improve the solution through correlation bounding.

The circular plots presented with each example portray rotor trajectories as seen by an observer looking along the -yaw direction in Fig. 2. Points are periodically plotted over the curves for identification purposes. The plotted saturation index has been adapted from the related discussion in Sec. 4.4 of Ref. 2, and is a quantity ranging from zero to one, representing the degree of momentum saturation in the CARES system (unity denotes saturation). The plotted gimbaling rates are scaled up by a factor of 100.

1) Momentum Saturate CARES System Along Pitch/Roll

The first set of examples to be presented illustrate the response of the CARES system to an input command sequence consisting of a monitonically increasing series of equal pitch and roll rate commands (yaw rate is held at zero). This sequence eventually drives the CARES system into momentum saturation.

The first example of this type commands a vehicle pitch/roll rate increment of 3 deg/sec every two seconds. Rotor angles are plotted in Fig. 3. The circular plot in the upper left corner summarizes the response; at first the two rotors originally at +pitch and +roll (starting positions are denoted by "S") were rotated about ϕ to the -pitch,-roll quadrant (the ϕ rotations are relatively inexpensive here; it is much more costly to increase θ). Since the CARES selection is updated frequently, the global rotor trajectories in this portion of the test are seen to follow constant θ latitude circles (as opposed to the great circle arcs individually pursued after each selection). After all rotors are brought into the same quadrant, roll/pitch torque is directly produced by increasing θ (remember that two rotors point up and two point down, thus this is a scissoring motion). As the rotors approach their stops, they are driven together in ϕ, and all point as closely as possible opposite to the commanded axis (pitch/roll), indicating momentum saturation (point F).

Rotor angles are plotted vs. time in the right-hand column, where we see that increases in θ were kept minimal while the rotors were re-distributed in ϕ. The composite gimballing rates (a_c) are plotted in the lower left. Here we see that the system stayed far from torque saturation, and typical gimballing rates were well below their maxima. The "sawtooth" appearance is due to the discrete rate steps input to the proportional controller (see vehicle rates in Fig. 4). This profile is seen to become more complex while the polar angles are being incremented after t=20 sec. This is due to "switching" of the linear solution; as some rotors are advanced to larger θ, their activity vectors become more expensive, thus other rotors are selected to be advanced in their place

until they achieve equal expense, and the cycle repeats again. In this fashion, the linear program discretely "steps" the rotors into the stops.

Because the torque requirements were low, the linear program was able to solve most commands with only three activity vectors in the basis (none were needed at upper bounds). This strategy contributed to the "switching" phenomenon mentioned above, and also created an effect noted in the polar plot of Fig. 1; ie. the gimbal trajectories are seen to generally follow coordinate axes ($\hat{\tau}_\theta$ or $\hat{\tau}_\phi$). The linear program tends to pick such rotor trajectories in this example because the calculated activity vectors are always aligned with coordinate axes, and only one activity vector is typically selected per rotor (due to the low torque requirement).

Fig. 4 shows the saturation index and vehicle rates. The linear increase of the vehicle pitch and roll rates in response to input commands (dotted staircase) drives the system progressively toward momentum saturation, as seen by the rise in the saturation index. By $t \approx 45$ sec, the CARES system has momentum saturated (sat. index = 1), and can no longer increment vehicle rates (due to the low inertias of the spacecraft, a hefty 70°/sec has been achieved at saturation). Although the linear program has the ability to introduce jets and continue to control the vehicle after this point, these simulations were not structured to exploit this feature.

The next application of this test sequence commands pitch/roll rate increases of 3 deg/sec every 0.3 sec. This will require considerably more torque authority from the CARES system than needed in the previous test. Rotor positions are plotted in Fig. 5. The circular plot shows a somewhat different response; because of the larger torque requirement, rotor trajectories no longer follow pure ϕ paths initially, but are moved much more directly toward -pitch,-roll. When all rotors are simultaneously in the -pitch,-roll quadrant, the polar angles are incremented together, and the system is driven toward momentum saturation.

Small limit-cycle oscillations are seen in the rotor ϕ-coordinates as the stop is approached. Since the maximum gimballing rates which increase θ are limited at large θ by the "soft stop" upper bounding

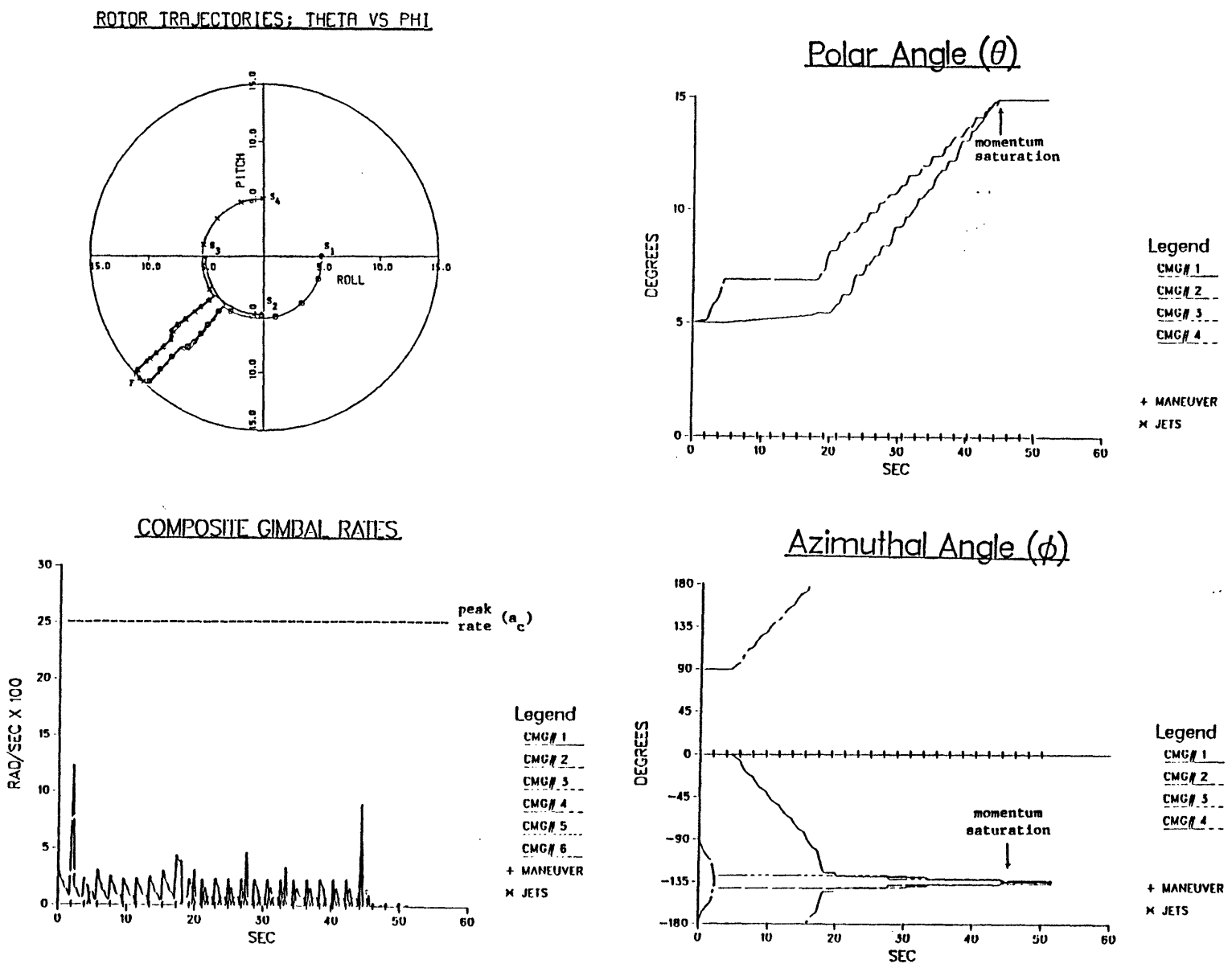

FIGURE 3: Momentum Saturate Along Pitch/Roll
Low Torque

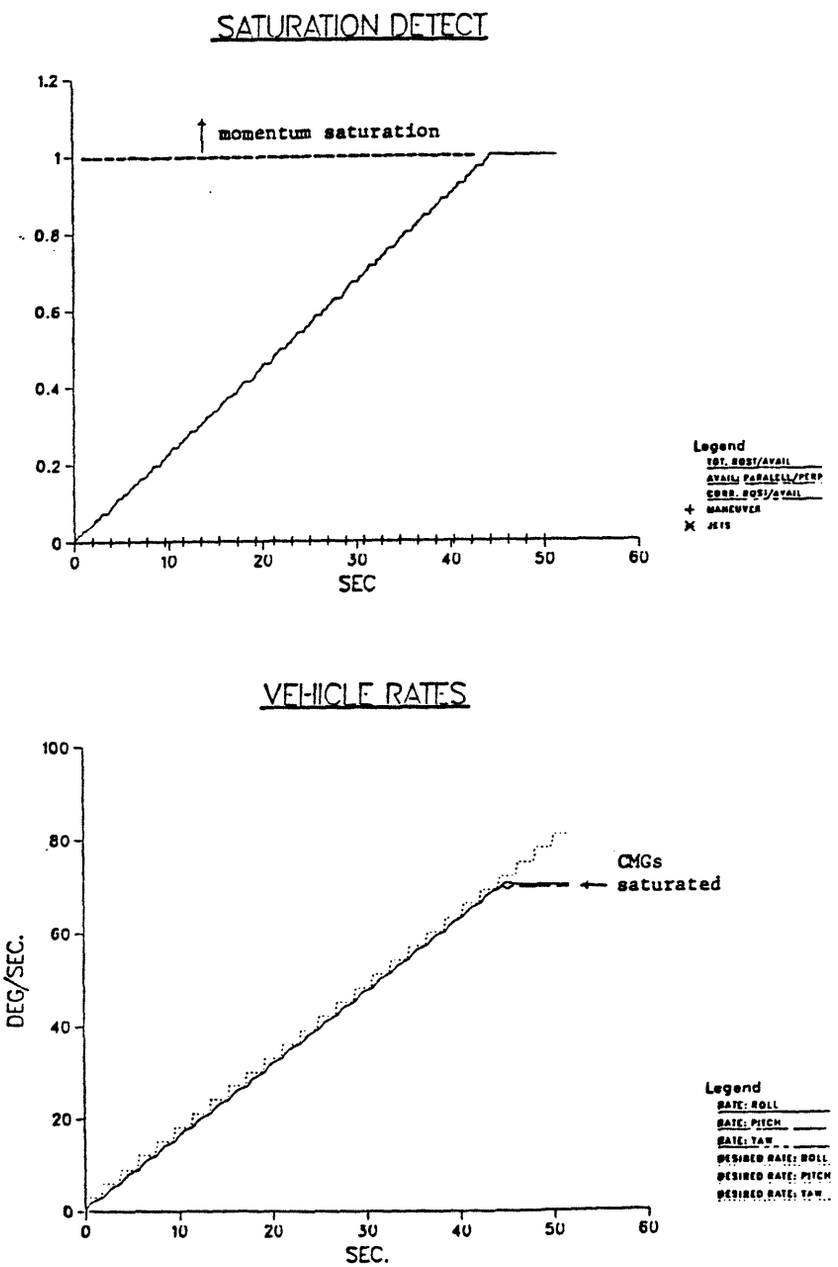

FIGURE 4: Momentum Saturate Along Pitch/Roll *Low Torque* (cont.)

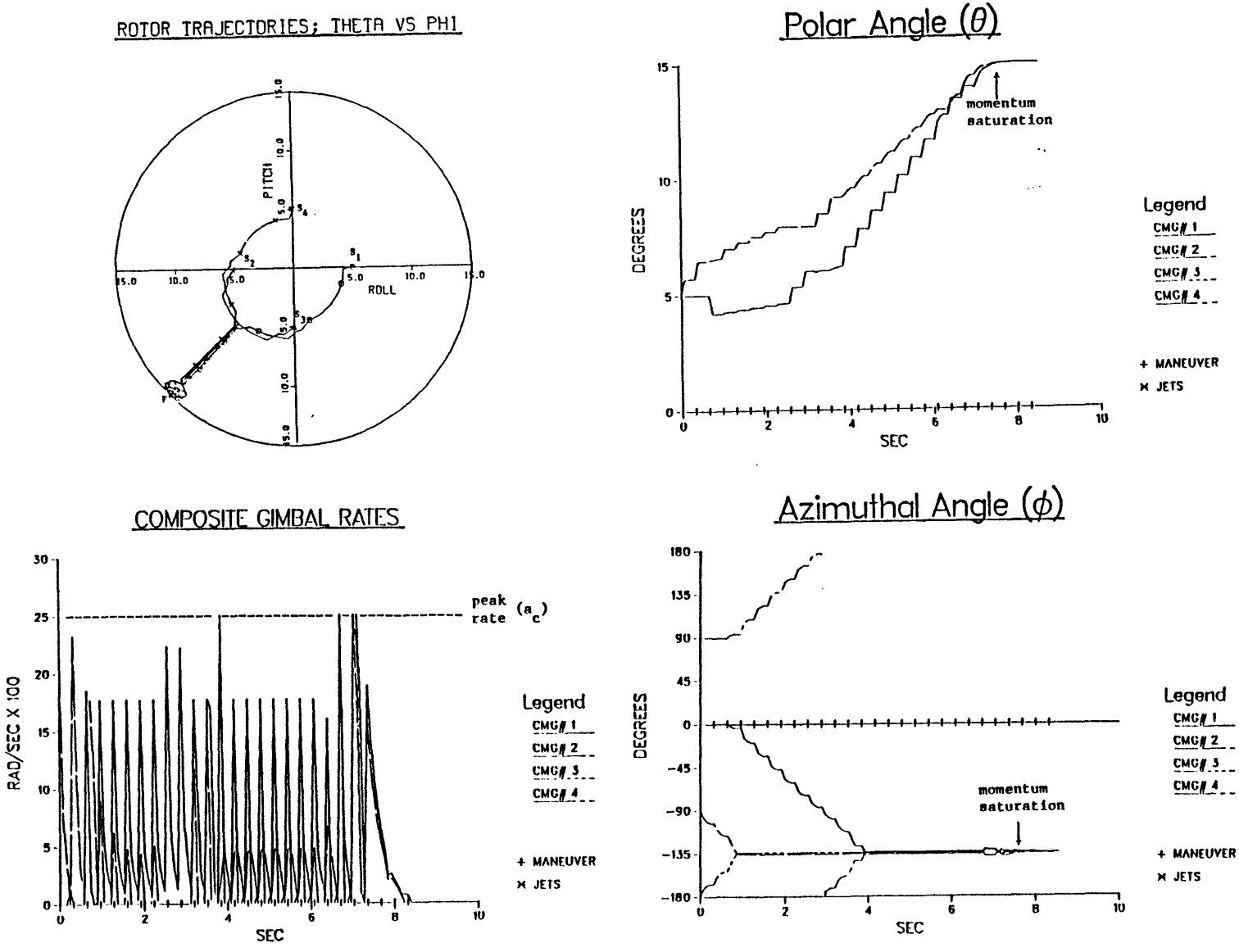

FIGURE 5: Momentum Saturate Along Pitch/Roll
Medium Torque

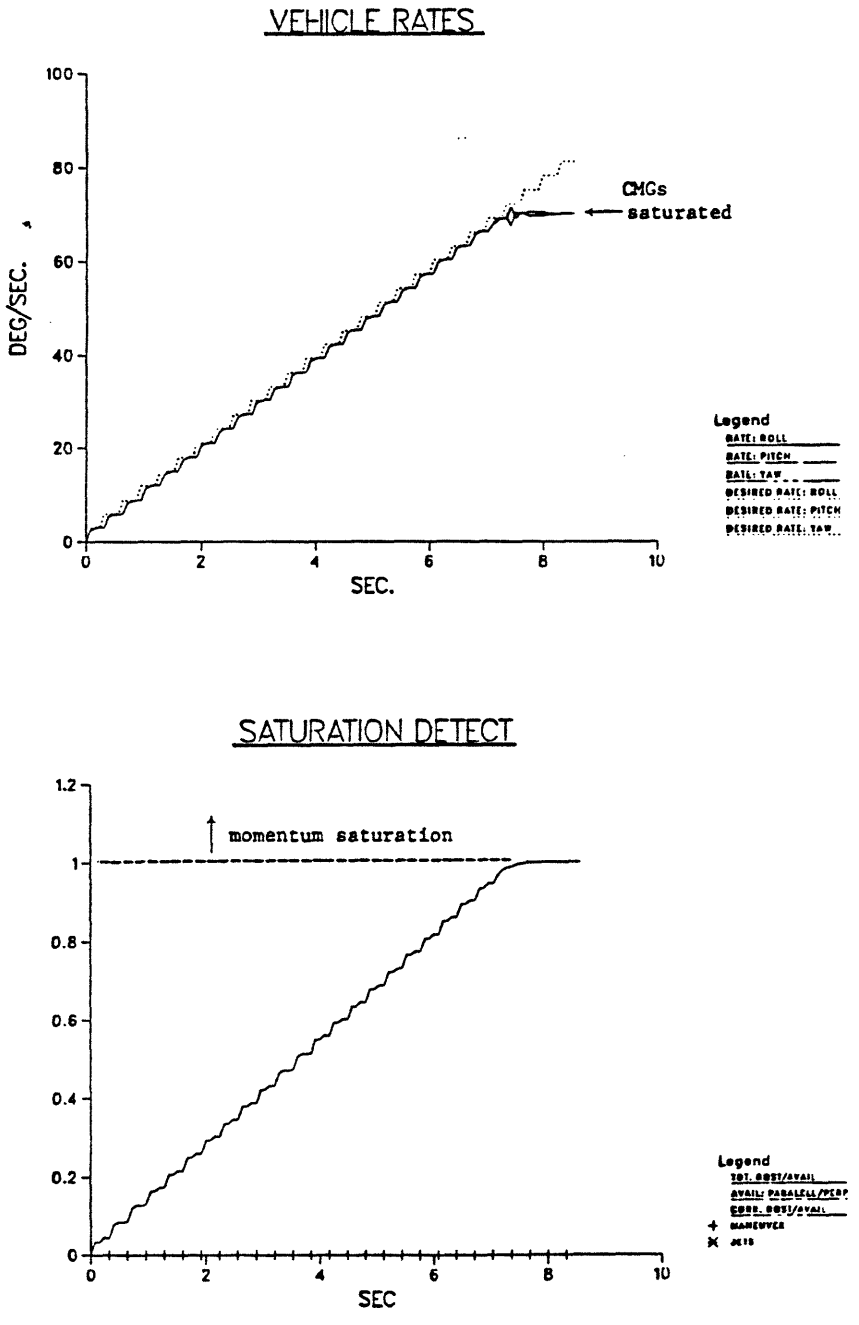

FIGURE 6: Momentum Saturate Along Pitch/Roll *Medium Torque* (cont.)

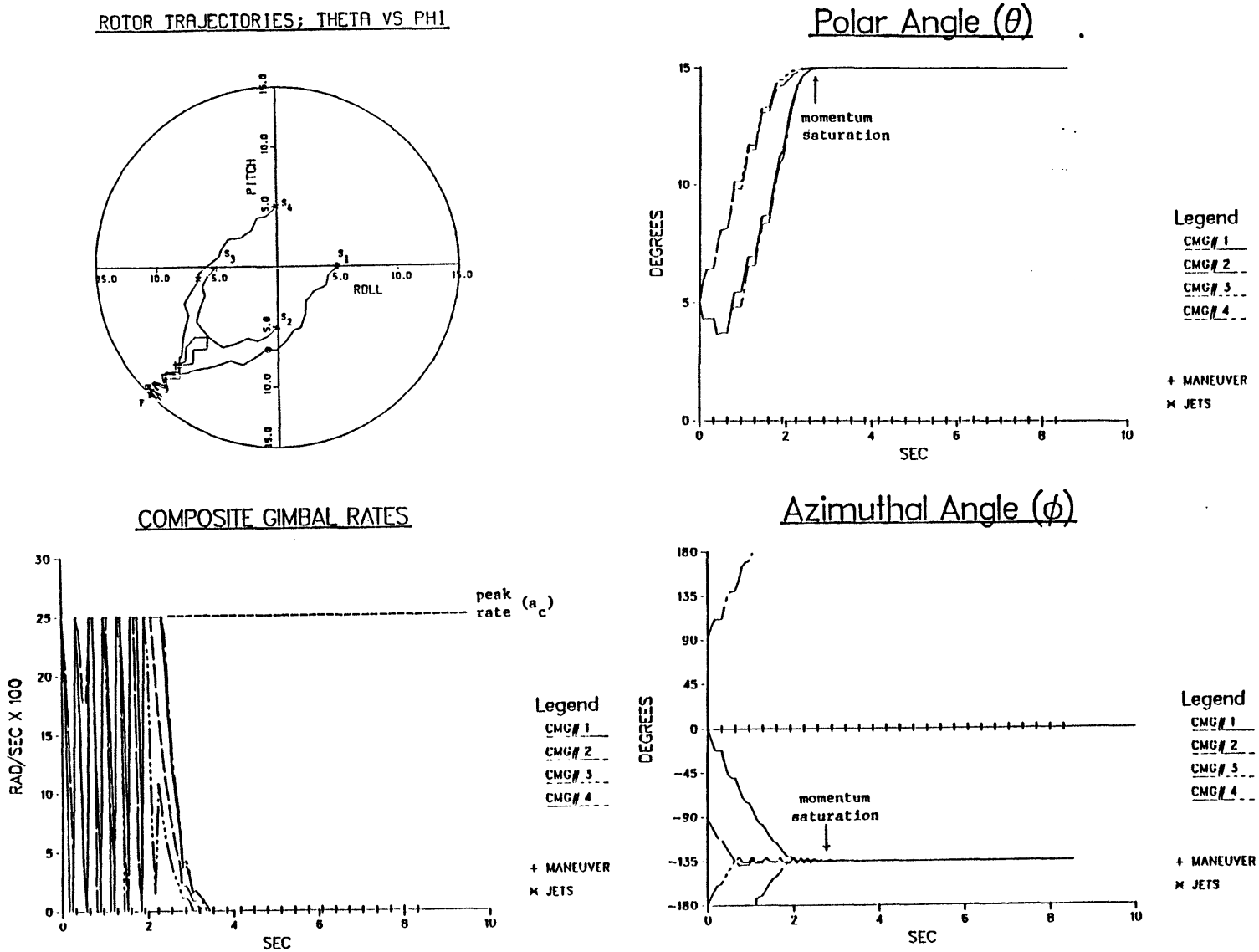

FIGURE 7: Momentum Saturate Along Pitch/Roll
High Torque

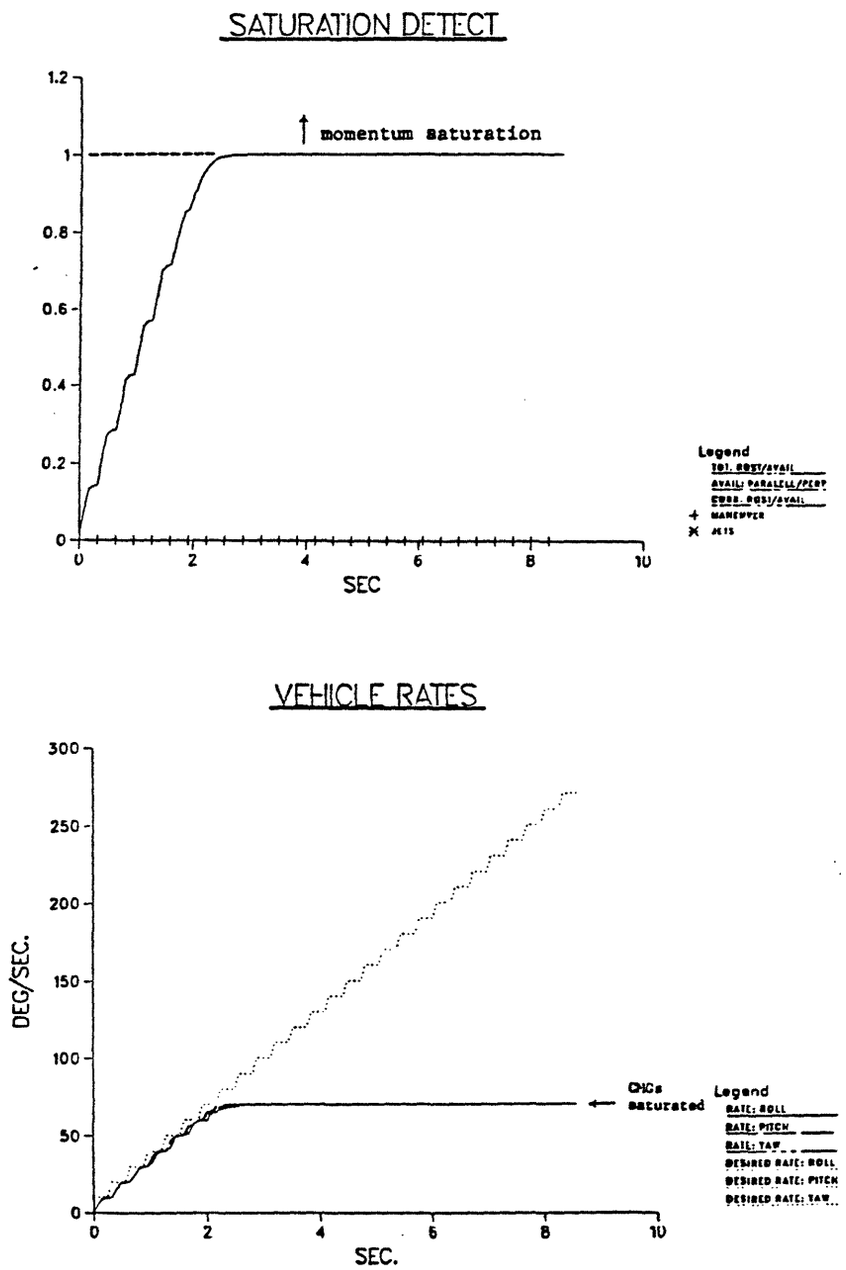

FIGURE 8: Momentum Saturate Along Pitch/Roll *High Torque* (cont.)

strategy (discussed in the previous section), the selection procedure attempts to derive additional control authority by moving the rotors in ϕ. Because of the high rotor rates and hysteresis introduced by the 80 msec controller update period, this causes limit cycling in ϕ centered about the -pitch,-roll axis.

Behavior of the individual polar and azimuthal trajectories vs. time are very similar to that seen in the previous example (except now the rotors are moving much faster). This is also noted in the plot of composite gimballing rate, where the standard sawtooth profile is noted to have much higher peaks. The composite gimballing rate never exceeds its maximum of 0.25 rad/sec; the only major interval where rotors were gimballed at this rate occurs at the conclusion of the test, where the "soft stop" strategy caused the ϕ limit-cycle oscillations discussed above.

The saturation index and vehicle rates are plotted in Fig. 6. The results are analogous to the previous example (Fig. 4), although the vehicle is now seen to respond much more quickly (the rate-change to torque gain of the proportional controller was increased in this example to achieve the higher torque level needed).

The final test in this series pushes the system at yet a much larger torque; rate-change commands of 10 deg/sec were input every 3 seconds. Rotor trajectories are shown in Fig. 7. The circular plot indicates an extrapolation of the behavior seen in the last two examples; the rotors are now pulled across as directly as possible to saturation at -pitch,-roll. Because rotors are now moving very quickly, the discrete controller update period of 80 msec becomes even more influential, and a much coarser rotor trajectory is noted, with increased limit-cycle oscillations in ϕ as the stop is approached. Composite gimballing rates are seen to be often at maximum (the rate bounding strategies discussed in the previous section prevent these limits from being exceeded), and the system is now frequently in torque saturation.

Figure 8 shows momentum saturation to be reached at t=2 sec (the time scale of these plots is the same as that used in the previous example). Vehicle rates are rapidly built until momentum saturation

prevents further response after reaching 70°/sec about pitch/roll (the requested rate continues to increase, as per the plotted dotted staircase).

2) Momentum Saturate CARES System Along Yaw Axis

The next test uses a sequence which commands vehicle rate increases of 0.3 deg/sec about yaw every 0.6 seconds. Because the CARES rotors are initially displaced only 5 degrees from the yaw axis, the control authority about yaw is severely limited, and the system saturates very quickly.

Rotor positions are plotted in Fig. 9. The circular plot summarizes the CARES response. The two rotors which point into the -yaw direction are moved directly into anti-alignment with the yaw axis (these rotors move along the pitch and roll coordinate axes, thus their trajectories can be discerned from these plots only by the plotted characters [+ and *]). The two rotors pointing along +yaw are simultaneously scissored directly toward the stop limits. The system finishes in saturation, with the lower two rotors pointing into -yaw and the upper two scissored apart (180° separated in ϕ) at the stop limit. This configuration has delivered as much momentum as possible into the +yaw vehicle axis. The controller continues trying to drive the system past saturation by limit-cycling the lower two rotors repeatedly past their maximum yaw projection. This behavior could be avoided in practice by stopping system activity at saturation (torque saturation is indicated by imaginary activity vectors in the simplex solution, and momentum saturation is associated with a rise toward unity in the saturation index).

Plots of rotor angles vs. time are given in the right-hand column. The saturation limit cycling of the two -yaw rotors about the yaw axis causes the disturbances seen after their trajectories approach zero polar angles. The small motion around zero in polar angle is translated to large swings in azimuth as ϕ abruptly transitions between +/-180°.

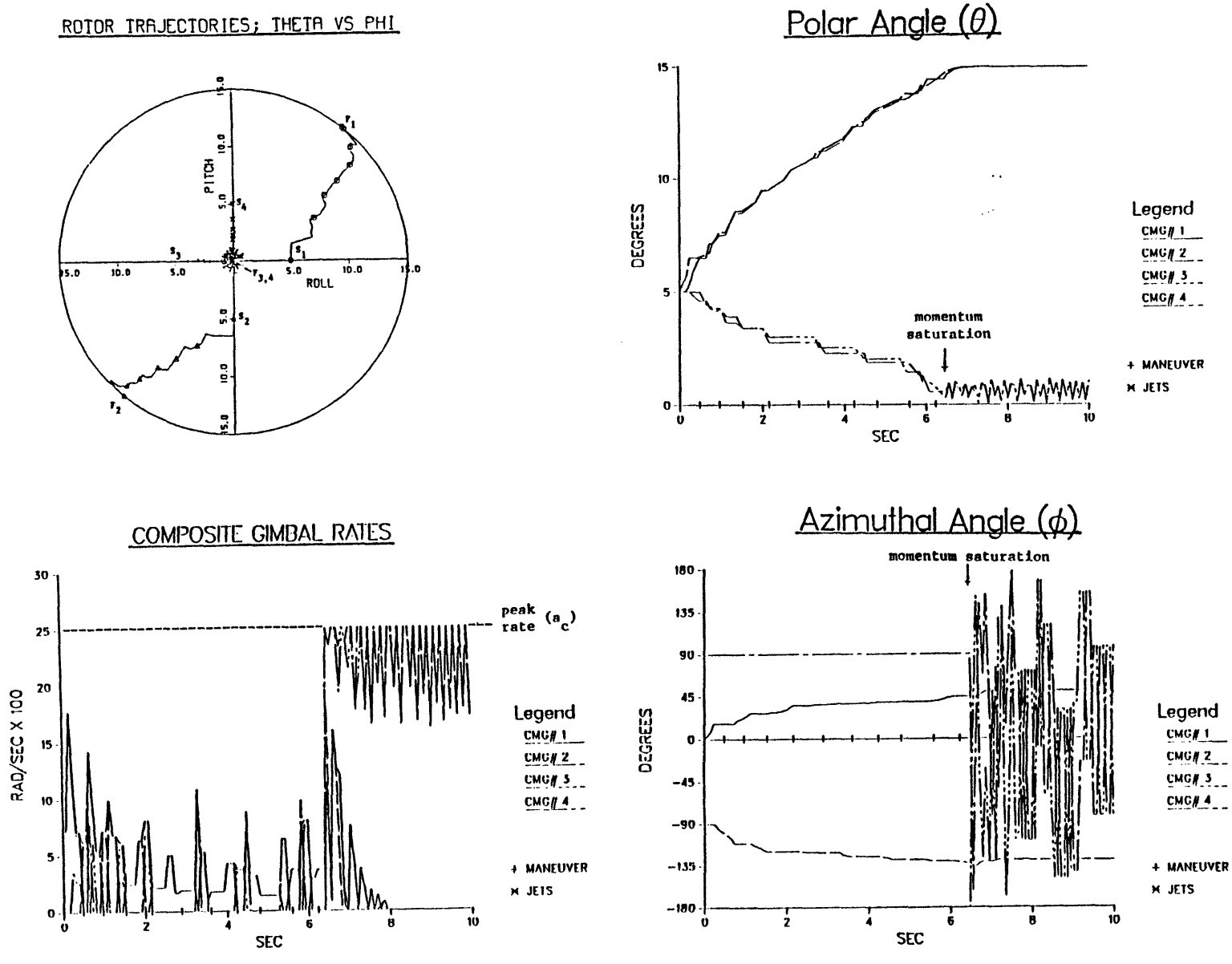

FIGURE 9: Momentum Saturate Along Yaw

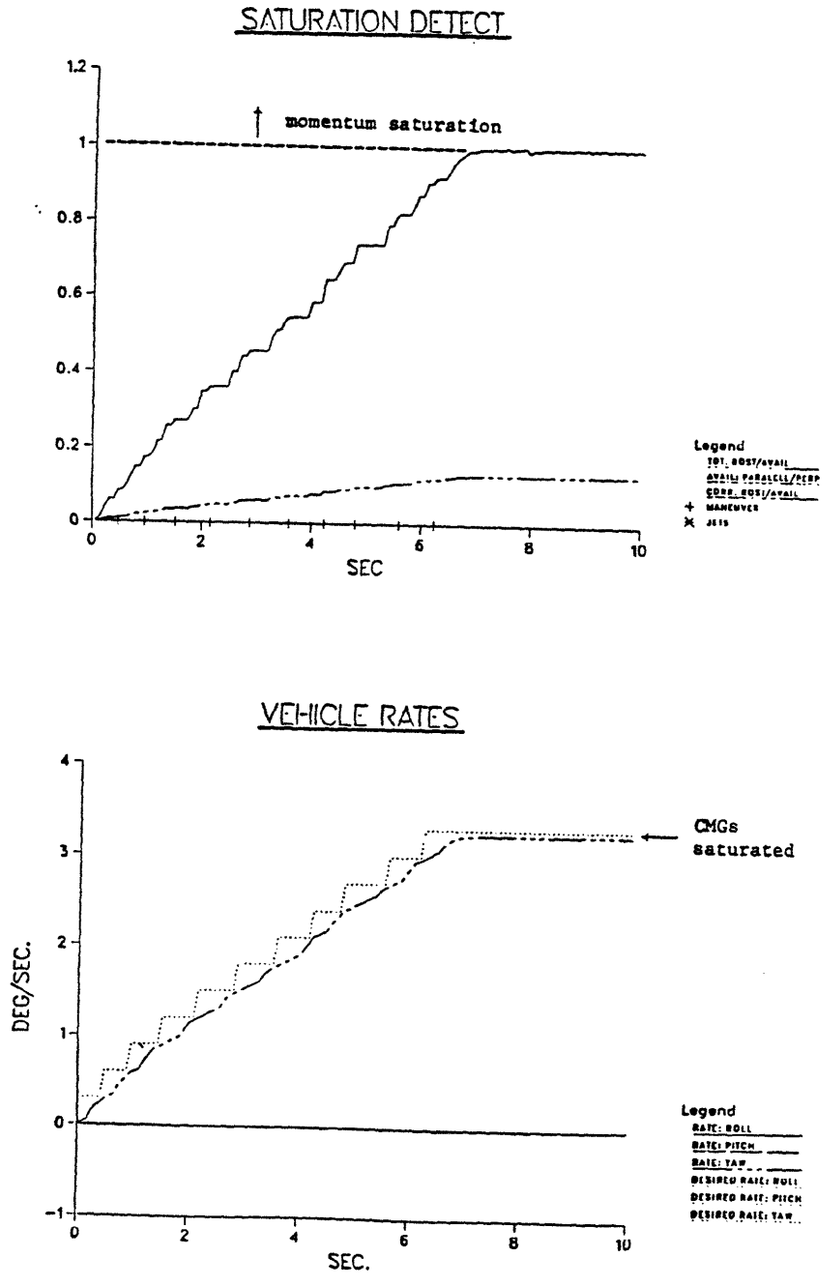

FIGURE 10: Momentum Saturate Along Yaw (cont.)

Gimballing rates are generally well below their maxima until saturation is reached, where the system futilely attempts to continue meeting input commands (note that the simplex bounding logic prevents the composite maximum of 0.25 rad/sec from being exceeded). This limit-cycling behavior may easily be avoided in practice, as discussed above.

Plots of the saturation index and vehicle rates are given in Fig. 10. Input commands are continually answered until the system reaches momentum saturation after attaining approximately 3.2 deg/sec about the vehicle yaw axis.

3) CARES Response to Rapid Attitude Slew in Pitch

The examples presented in this section illustrate the response of the CARES system to an attitude step commanded about the vehicle pitch axis. The mission directive summarized in Ref. 4 indicated the necessity of performing a five degree slew within one second. This implies a considerably higher controller and environment update interval than the 80 msec period assumed in the previous tests. In the following examples, the vehicle environment was updated every 5 msec, and control was applied with a similar frequency. In practical applications, a controller with this degree of complexity would not be iterated so quickly; the high update rate was chosen to examine the performance of the CARES steering procedure under ideal conditions, ie. minimizing hysteresis effects as seen in the high torque examples presented in the first group of tests.

The first example in this section achieves this attitude change by commanding a 10°/sec rate (at low torque) about the vehicle pitch axis. As seen in the rotor angle plots of Fig. 11, this rate is built and removed primarily by scissoring the rotors in the azimuthal direction. Little polar angle involvement (which can be more costly) is attempted. The plot of composite gimballing rates shows that no rotors were gimballed at the maximum limit, thus the system did not torque saturate. The high controller bandwidth is evident in the rapid changes seen in the

commanded gimballing rates; a dynamic model corresponding to the actual hardware behavior may well preclude such a prompt response.

The saturation index is plotted in the upper portion of Fig. 12, where it is noted that this maneuver only required approximately 10% of the peak system momentum capacity. The vehicle rate is plotted below, where the 10 deg/sec command was attained and removed both within 0.5 second intervals. This smoothly achieved the desired 5° pitch increment, as noted in the lower plot of resulting vehicle attitude.

The next example also achieves the 5 degree pitch maneuver by commanding a 10°/sec rate. Now, however, the CARES system is commanded to provide more torque such that the peak rate is attained in 0.25 sec (half of the time required by the previous test).

Rotor trajectories are shown in Fig. 13. The general appearance is similar to that seen in the previous example, except more polar angle involvement is noted. The mixture of polar and azimuthal rotor motion seen in the circular plot is more clearly understood when one remembers the fact that the vehicle is actually controlled along three axes. This plot is a flat projection onto the pitch/roll plane. The actual motion of the rotors will produce finite yaw torque, which must be compensated by additional azimuthal or polar rotor displacement. As seen in the lower left plot, gimballing rates are somewhat higher because of the larger torque requirement, and reach their peak values only at the beginning of the acceleration and decelleration phases.

Because the coast rate is identical to that achieved in the previous test, the CARES system is seen to approach the same degree (10%) of momentum saturation (Fig. 14). The vehicle rate is indeed noted to be built and removed twice as promptly, due to the increase in commanded torque. The lower plot of Fig. 14 shows the desired five degree pitch slew to be satisfactorially attained well within the alloted one second interval.

The final test of this section also commands an attitude slew in pitch. The demands on the system are now much stronger; a vehicle rate of 90°/sec is built and removed within alloted 2.5 sec intervals. Rotor trajectories are shown in Fig. 15. The rotors are first all moved into

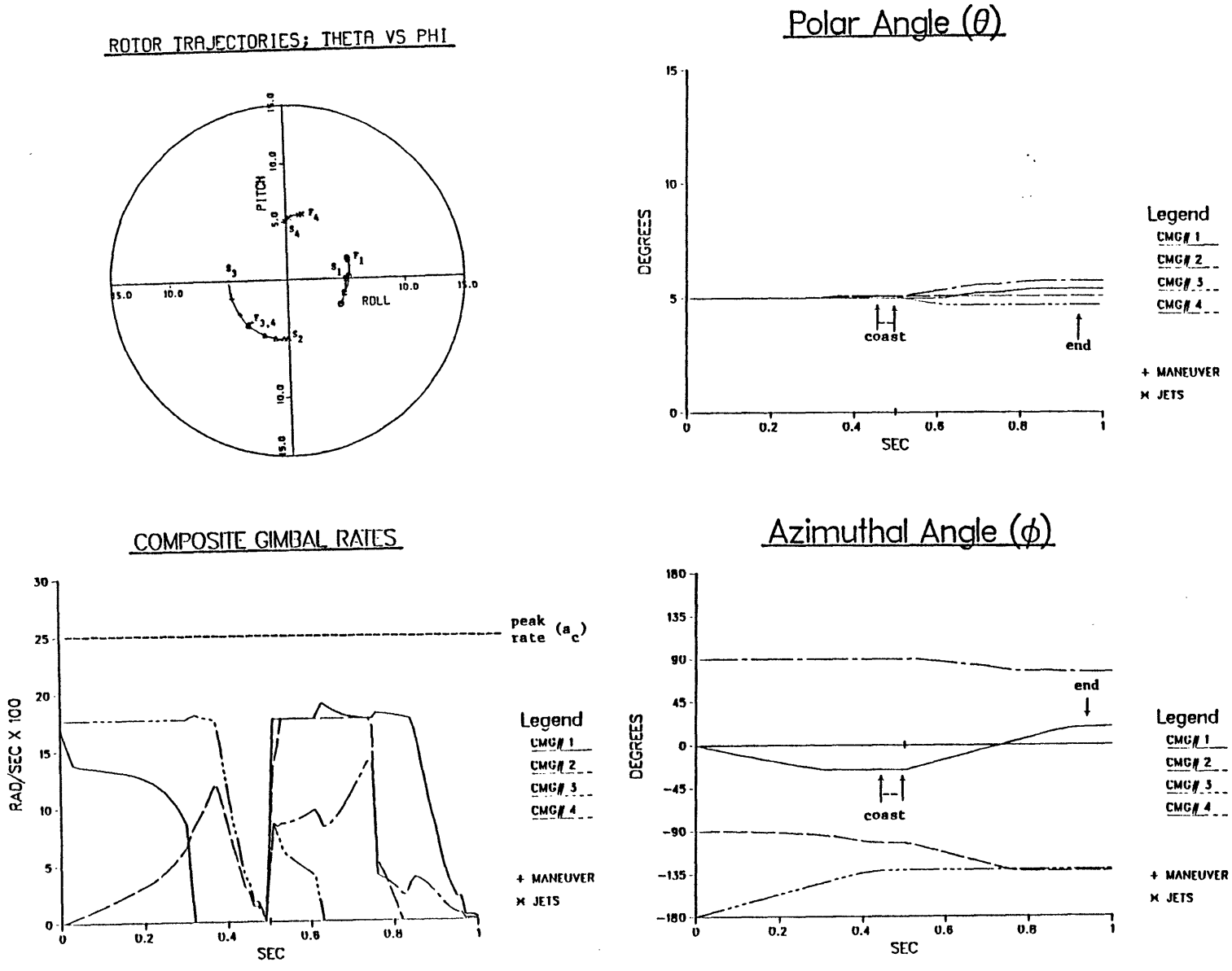

FIGURE 11: Rapid Attitude Slew in Pitch
Low Torque

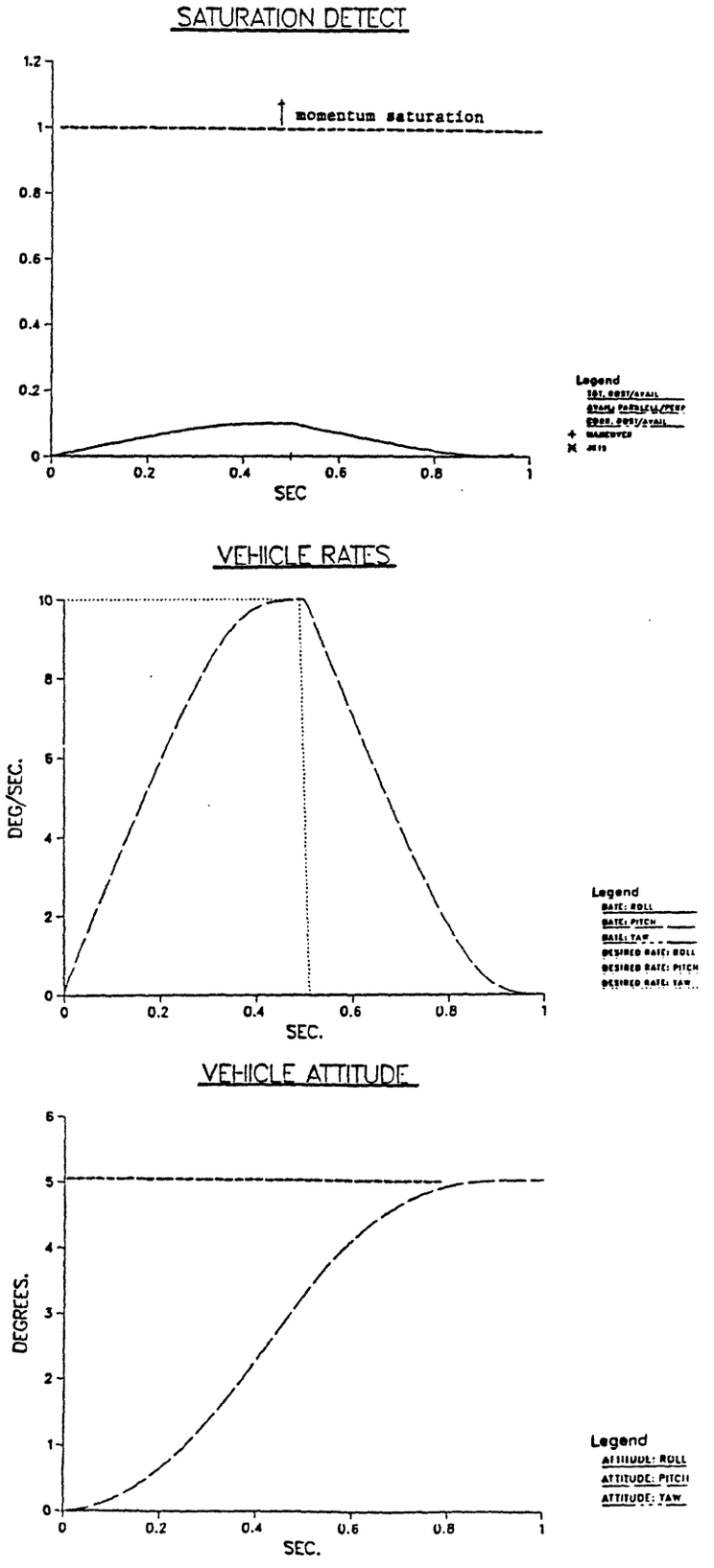

FIGURE 12: Rapid Attitude Slew in Pitch
Low Torque (cont.)

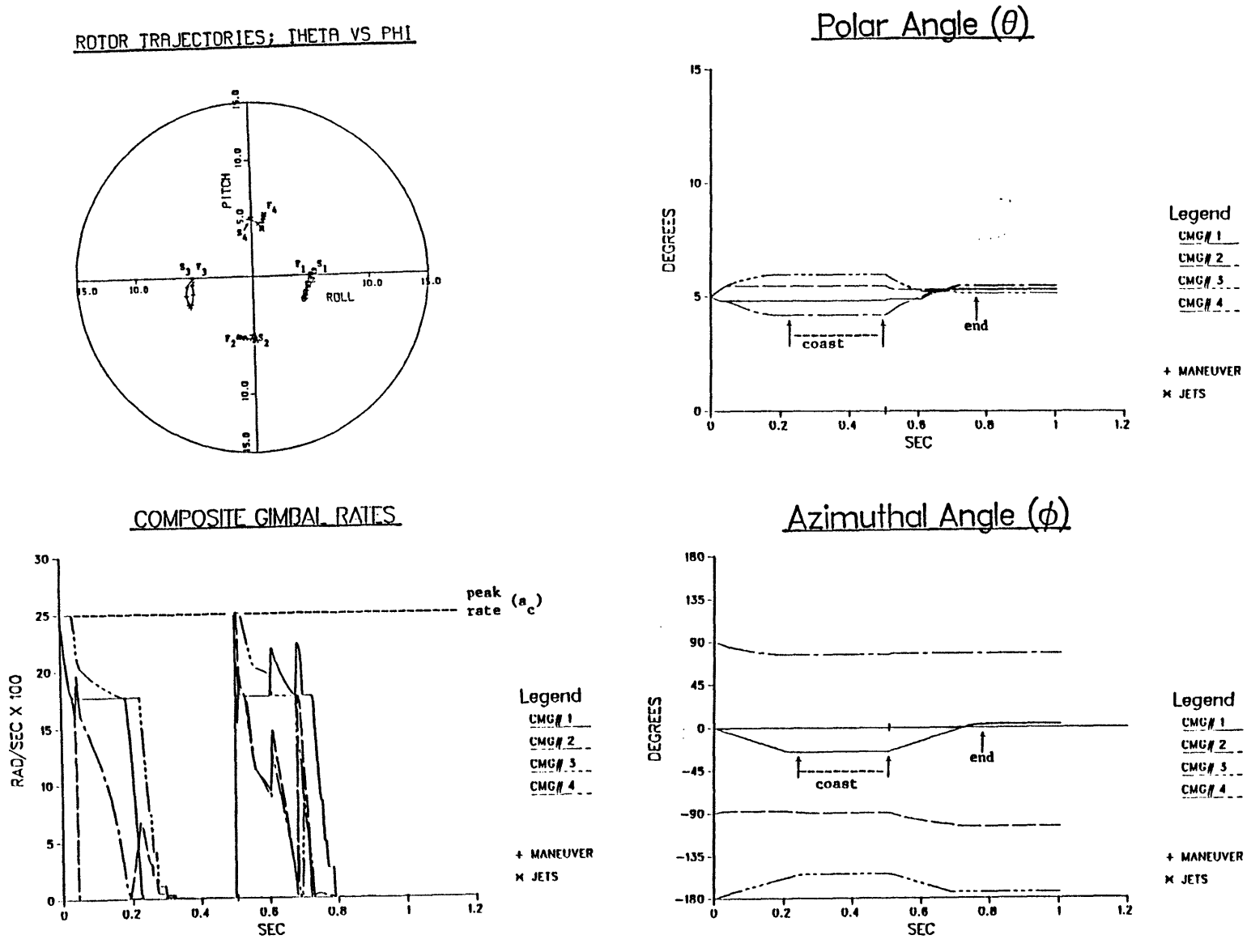

FIGURE 13: Rapid Attitude Slew in Pitch
Medium Torque

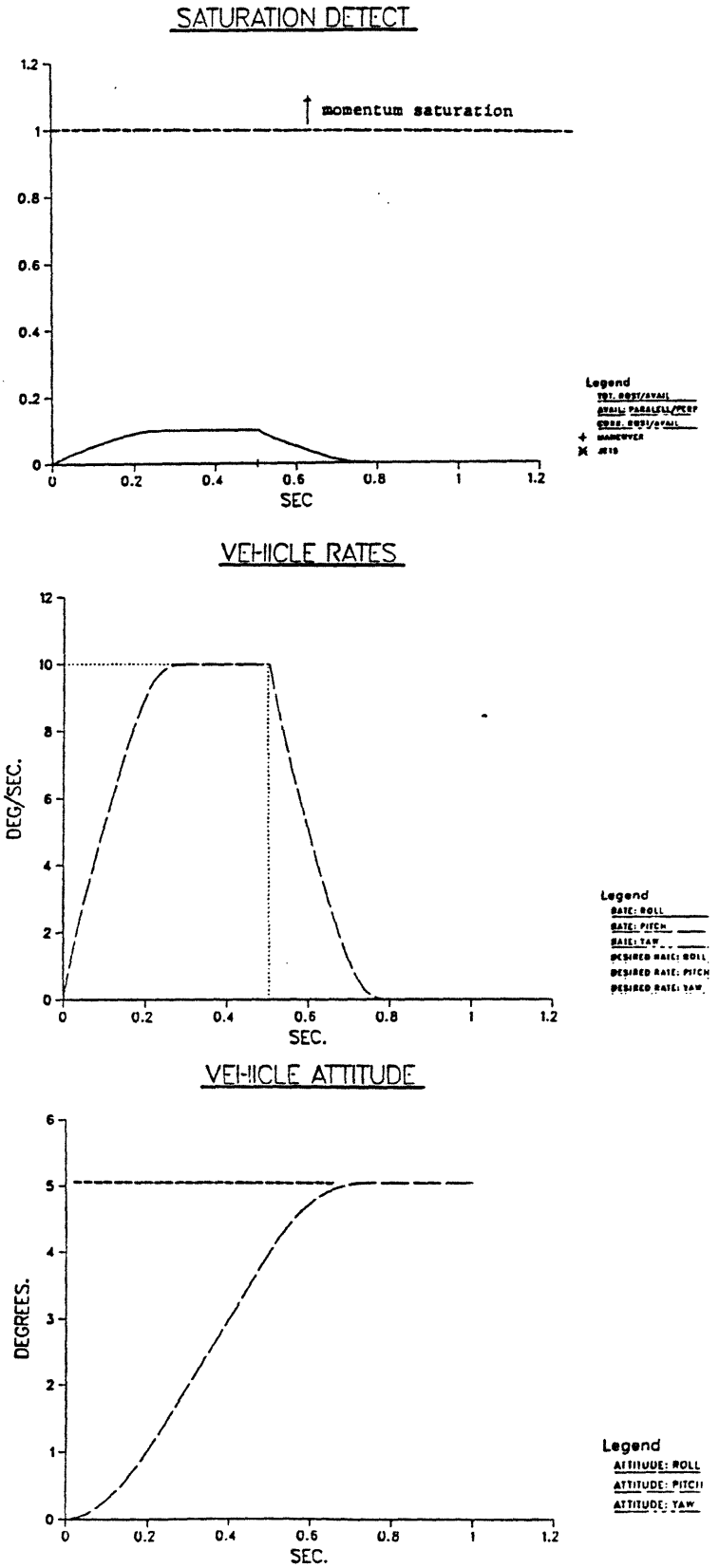

FIGURE 14: Rapid Attitude Slew in Pitch
Medium Torque (cont.)

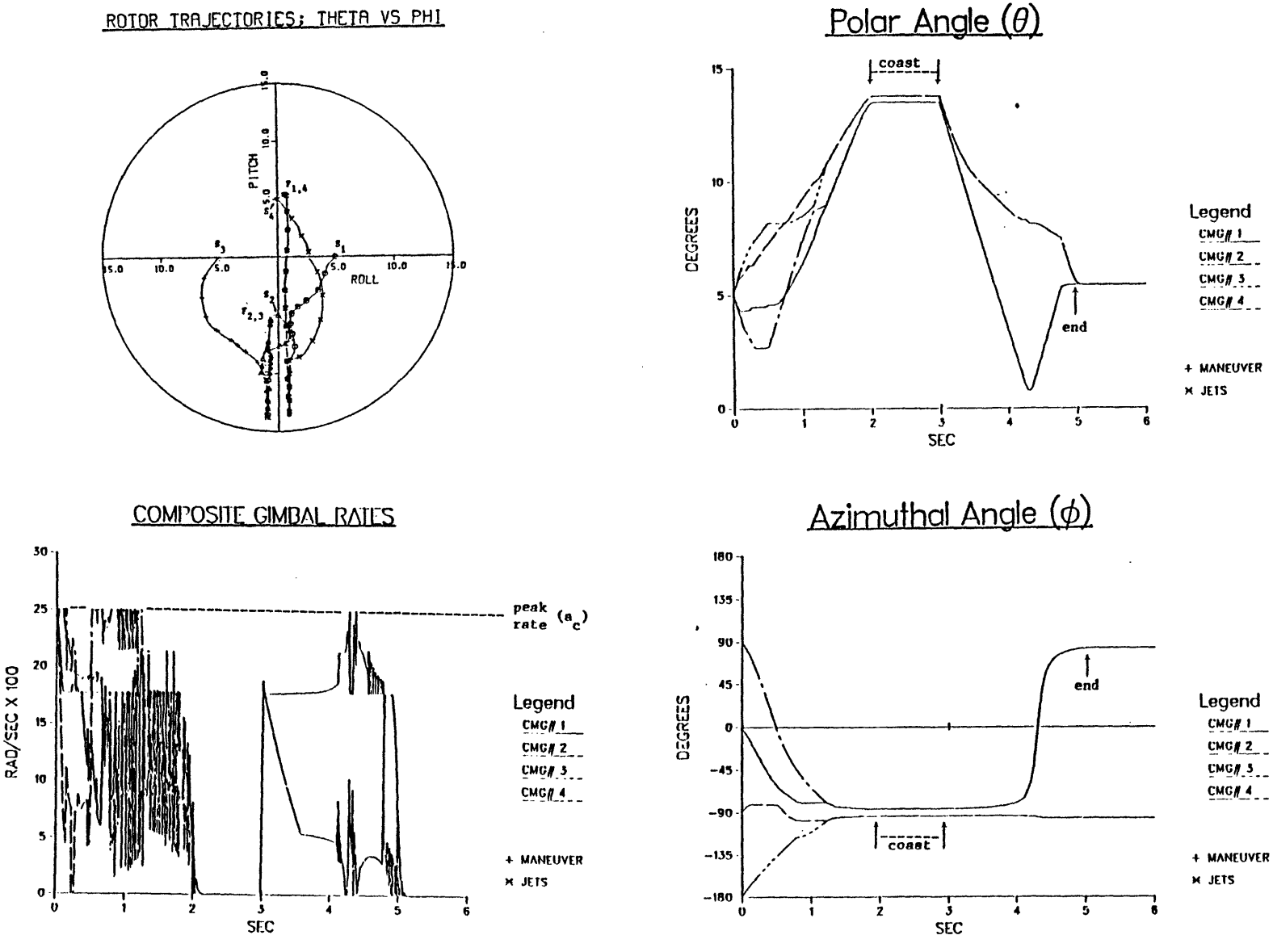

FIGURE 15: Rapid Attitude Slew in Pitch
High Torque

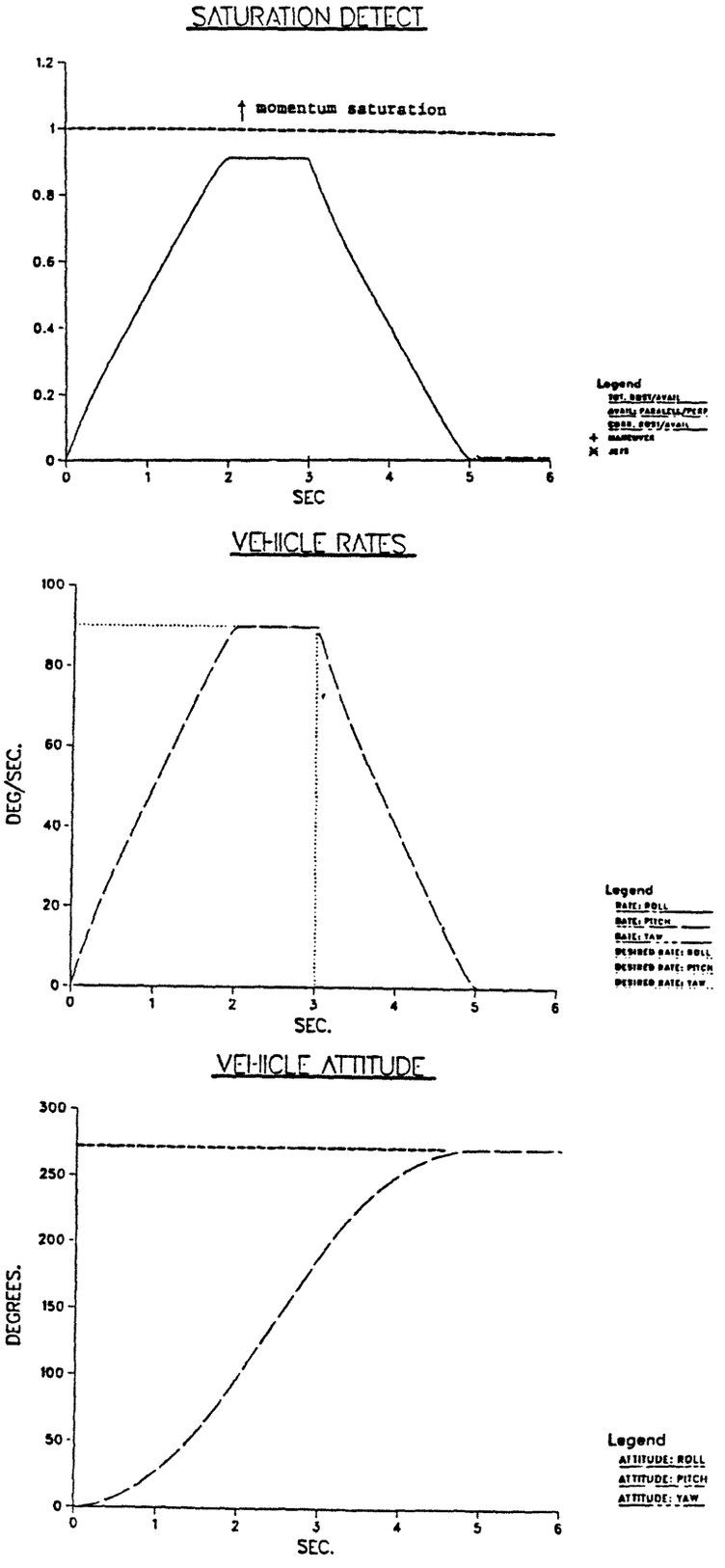

FIGURE 16: Rapid Attitude Slew in Pitch
High Torque (cont.)

the -pitch hemisphere (the non-direct trajectory is taken, in part, to maintain zero yaw torque while building vehicle rates about pitch), and subsequent pitch torque is achieved by increasing polar angles to move rotors toward the -pitch axis. The rotors are returned to a zero momentum state primarily through polar motion; two sets of two opposing rotors each are returned together to form pairs scissored by 5° and oriented back-to-back. The zero-momentum simultaneous 4-rotor alignment state is avoided, as encouraged by the anti-lineup objective contribution.

Considerable oscillation is seen on the composite gimballing rates, primarily in the portion of the trajectory which builds the desired vehicle rate. This is due to the polar angle "stepping" effect discussed earlier. Because of the changes in objective function arising from the increasing expense of advancing polar angles, the linear program often revises its solution (indicating which rotors are advanced with what rates) at every selection. Since the controller update rate is so high here (ie. 5 msec), the solution is changed very frequently while advancing polar angles, giving rise to the noisy appearance of the net gimballing rates. Physical actuators would not be fed such a signal; a light filtering operation could easily remove this effect (the gimbaling rates are integrated in the plots of CARES rotor angles, which are indeed quite smooth in the oscillatory regions). Because of the correlated bounding scheme, gimballing rates are never seen to exceed their maximum limit.

As seen in Fig. 15, the system now approaches momentum saturation much more closely (ie. over 90% of the system capacity is used). This is required by the commanded 90 deg/sec vehicle rate, which is seen to be promptly attained and removed in the middle plot of Fig. 15. The lower portion of the figure shows the vehicle attitude, which has changed in pitch by 270° within 5 seconds.

V) Conclusions

The purpose of this study has been to investigate the incorporation of a magnetically suspended CARES gyroscope into the linear programming based hybrid actuator management procedure described in Refs. 1 and 2. The strategy applied to divide the output torque into orthogonal components (thus creating a set of virtual gimbals and activity vectors for simplex selection) provided an effective means of allowing the simplex process the ability to specify the direction of rotor displacement. Methods of driving the CARES system were discussed that attain a commanded rate change or desired torque. The gimbal stop location was incorporated into the upper bounding structure of both scenerios. In response to an input torque command, two strategies were presented to bound the quadrature sum of the decision variables corresponding to the orthogonal components of rotor gimballing rates. One method restricted each component of rotor motion to remain below the peak limit divided by $\sqrt{2}$. The other involved dynamically altering the simplex upper bounds while the problem is being solved. Both of these techniques have disadvantages, however, that can prevent the maximum system torque output from being projected along the commanded axis in certain cases. Strategies to improve these techniques were outlined; these generally involve incorporating the orientation of the input request into the upper bound calculation, or re-working the simplex procedure to avoid "pivoting impasses" caused by the correlation limits. Because of the limited nature of this preliminary effort, these concepts could not be investigated in any detail; any future work which is performed in this area may draw upon this experience to achieve improved results.

Since a magnetically suspended rotor possesses no "hard mount" to the host spacecraft, the rotor position must be maintained relative to the spacecraft by additionally driving the torquing coils while the vehicle is rotating (ie. all effective rotor torques must be applied relative to inertial space; even if no gimballing rate is commanded in body coordinates, the rotor axis must still be driven to null the precessional torques caused by vehicle rotation). Because of this, the

actual peak "gimballing rates" possible to apply in spacecraft coordinates may vary with gimballing direction and vehicle rate. This should be considered in any subsequent efforts which involve a more detailed hardware model.

A series of simulation examples were presented that illustrate the response of a CARES system to command sequences which perform rapid slews in vehicle attitude, or increase vehicle rates until momentum saturation is reached. The CARES system defined in the simulation was seen to successfully meet all mission objectives, and the linear selection was able to consistantly specify CARES responses that maintained vehicle control at several different levels of commanded torque. The unique abilities of linear programming to adapt to arbitrary device definitions and failure modes (as demonstrated in Refs. 1 and 2) can also be exploited by a CARES system, creating a highly adaptable CARES control package.

The examples contained in this report demonstrate successful vehicle control achieved with an array of CARES gyroscopes. The simple kinematic device model used in this study, however, does not assume any transients or noise in the hardware response. Any future investigations should incorporate a more realistic dynamic hardware model in order that actuator behavior is better simulated; this is particularly important to maintain the veracity of rapid slew and precision pointing studies, where dynamic effects and actuator noise can significantly affect performance.

VI) References

1) Paradiso, J.A., "A Highly Adaptable Steering/Selection Procedure for Combined CMG/RCS Spacecraft Control," Proc. of the 1986 American Astronautical Society Rocky Mtn. Guidance & Control Conf., AAS-036, Feb., 1986.

2) Paradiso, J.A., "A Highly Adaptable Steering/Selection Procedure for Combined CMG/RCS Control; Detailed Report," C.S. Draper Lab. report CSDL-R-1835, March, 1986.

3) Eisenhaure, D.B., Downer, J.R., "Study of a Combined Attitude, Reference, and Energy Storage (CARES) System,", Contribution to the 1985 C.S. Draper Laboratory Technical Report from IR&D Project 171, pp. 195-221, July, 1984.

4) "Space Relay Experiment; Definition Phase Status Review," NASA/JPL report, June 27, 1986.

5) O'Dea, S., "Steering Laws for CARES Actuator," CSDL Internal memo MSD-2173-86, July 21, 1986.